New speckle analysis algorithm for flow visualization in Optical Coherence Tomography images

Lucas R. De Pretto, Gesse E. C. Nogueira, Anderson Z. Freitas
Nuclear and Energy Research Institute, IPEN–CNEN/SP, Av. Prof. Lineu Prestes 2242, São Paulo, SP, Brasil 05508-000;

ABSTRACT

Optical Coherence Tomography (OCT) is a noninvasive technique capable of generating in vivo high-resolution images. However, OCT images are degraded by a granular and random noise called speckle. Nevertheless, such a noise may be used to gather information regarding the sample, as is exploited by techniques like Speckle Variance – OCT (SV-OCT). SV-OCT is widely used in the literature, but the variance calculation is computationally expensive. Therefore, we propose a new algorithm to employ speckle in identifying flow based on the evaluation of intensity fluctuation between two consecutively acquired OCT images. Our results were compared to those obtained by traditional method of Speckle Variance to demonstrate the feasibility of the technique. Both algorithms were applied to series of OCT images from a microchannel flow phantom, as well as from a biological tissue with blood flow. The results obtained by our method are in good agreement with those from SV-OCT. We've also analyzed the performance of both algorithms, registering the processing time and memory use. Our method performed 31% faster with the same use of memory. Therefore, we demonstrated a new method to map flow on OCT images.

Keywords: OCT, Optical Coherence Tomography, speckle, microflow, flow mapping.

1. INTRODUCTION

Optical Coherence Tomography (OCT)[1] is a contactless, noninvasive imaging modality that generates high resolution cross-sectional images of scattering media. It's penetration depth is dependent on the wavelength used, as well as the sample absorption. For biological tissues, the penetration usually is in the order of a couple millimeters[2]. Being an interferometry-based technique, the coherence in which it relies on also gives rise to a granular and high contrast noise, called speckle.

Speckle arises in OCT as a consequence of the latter sensitivity to the phase of the cross correlation between the optical fields returning from the reference arm and the sample arm. The main sources of speckle in OCT are multiple backscattering and delays caused by forwarding scattering inside the sample[3]. As a noise, speckle degrades OCT images quality, and great effort is put into trying to remove it[4-6]. However, being dependent on the scatterers inside the sample, whether those scatterers are moving or static affects the behavior of the speckle pattern through time. When it is originated by moving scatterers, this pattern presents more fluctuations of intensity over time (time-varying speckle), and, therefore, decorrelates faster, than when it comes from a static source. That provides a way to differentiate between the two regimens and use speckle as a source of information. One way to do so was proposed by Mariampillai et al. [7], known as Speckle Variance OCT (SV-OCT).

SV-OCT tries to differentiate the patterns of speckle by calculating the variance of every pixel in a series of sequential OCT images in time. It has since been utilized in many applications to visualize microflow[8-10]. However, its applications are limited to mapping of the underlying flow, not being able to characterize such a flow, as the literature reports SV as a qualitative rather than quantitative technique[11]. Also, the variance computation is computationally expensive when implemented using the naive method. In that way, it may be an unjustified complex algorithm to evaluate intensity fluctuations.

Therefore we propose a new technique that is also based on speckle and evaluates the intensity fluctuation on short windows of time, instead of analyzing a pixel intensity over all the acquired images in a single pass. We've implemented both algorithms and tested them with the same dataset of OCT images. In this work, we evaluate and compare the results obtained from both approaches, as well as analyze their performance in terms of processing time and memory usage.

Biophotonics South America, edited by Cristina Kurachi, Katarina Svanberg, Bruce J. Tromberg, Vanderlei Salvador Bagnato, Proc. of SPIE Vol. 9531, 95313O · © 2015 SPIE
CCC code: 1605-7422/15/$18 · doi: 10.1117/12.2180811

2. MATERIALS AND METHODS

Experimental Setup

For the experiments performed, a Fourier Domain OCT, the OCP930SR (Thorlabs, Newton, New Jersey, USA) was used, with a central wavelength of 930 nm, axial resolution of 6 µm in air and a declared axial digital resolution of 3.088 µm per pixel. For control of microflow, a syringe pump, the ExiGo (Cellix, Dublin, Leinster, Ireland) was used. This pump can be remotely controlled and generates flow rates ranging from 10 nL/min up to 20 mL/min. The microfluidic devices used in this work were Vena8 Fluoro+ (Cellix, Dublin, Leinster, Ireland), each chip counting with 8 rectangular microchannels, and each microchannel has width of 400 µm, height of 100 µm and length of 2.8 cm. Finally, as scattering media for the flow, whole milk (3% fat) was pumped through the microchannels.

The microfluidic device was positioned so that the milk would flow with a 90 degrees angle from the imaging beam and along the longitudinal (z) direction of the imaging plane. Therefore, the images are composed of a transversal cross section of the microchannel. This setup can be seen in Figure 1.

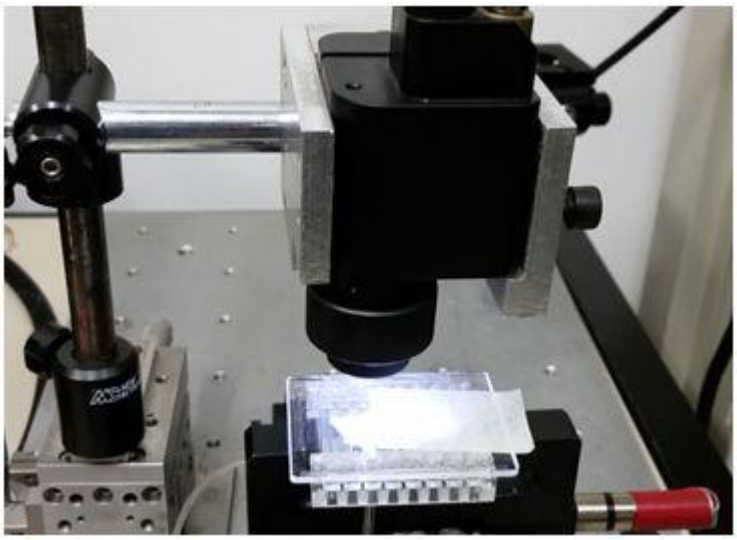

Figure 1. System and sample setup.

The acquisition software used is that provided with the OCT system. The B-Scans are acquired in raw data format, so the intensity values are not normalized for display, as in the case of an image format

Data Analysis

Basically, SV-OCT exploits the fact that, in flow regions, scatterers that cause speckle are in motion. As the OCT image is a cross section, an image representing the profile beneath a single lateral line of the sample, when such a B-Scan is acquired, a certain group of scatterers was below this line and contributed to the speckle pattern observed. However, when the scan is repeated, and a new B-Scan is acquired on the same line, the group of existing scatterers below it is not the same, or is not in the same position, and the pattern of speckle is altered. In regions without flow, the pattern remains with little to no changes, because there is no movement of the scatterers.

If multiple B-scans of the same position are acquired sequentially, each will contain a slightly different speckle pattern in the areas of flow, while in other areas this pattern remains correlated. One can then combine the data from these images, obtaining information about the existing flow regions in the sample.

One way to evaluate this data, in order to map the location of flow areas, is to calculate the variance of the intensity at a given point - a pixel - through a collection of images acquired sequentially.

The variance indicates how spread a set of values is around its mean. Because no flow regions have few intensity fluctuations, the intensity of a pixel in a given image is close to the average value of this pixel from the entire collection of images, and the variance is small. Conversely, in flow regions, as mentioned, these fluctuations will be constant and the average intensity is no longer a good representative for any particular image, as the values will be

widely spread, with a large variance. This analysis method is the main idea behind Speckle Variance OCT. If *N* B-Scans, or frames, are obtained at different times *t* (*t* varies from 0 to *N*-1), the variance in a given pixel *i, j* (*i* = lateral position, *j* = depth) can be obtained by the following equation:

$$SV_{i,j} = \frac{1}{N}\sum_{t=0}^{N-1}\left(I_{i,j,t} - \langle I_{i,j}\rangle\right)^2 \quad (1)$$

Where $I_{i,j,t}$ is the intensity of the pixel *i, j* at time *t*; and $\langle I_{i,j}\rangle$ is the average intensity of the pixel *i, j* throughout *N* frames. The results of variance for each pixel obtained from these N B-Scans generate one new image, false color coded (grayscale) based on the variance value. Thus, pixels having large intensity fluctuations result in a brighter pixel (higher value) in the resulting image, while pixels with little or no fluctuations generate a darker pixel (lower value).

However, it could be argued that, since the SV technique does not provide any quantitative information about the flow, being only qualitative, the algorithm used is computationally expensive, demanding high processing time.

In order to speed up the generation of flow maps, and simplify the type of calculation used, it is propose here a new algorithm to separate fixed targets from moving ones. This algorithm takes advantage of the same factor that influences the SV - in the areas of flow speckle presents, in time, a wider range of intensities than the static areas.

It is argued be possible to discern between the two regimes noting only the change in intensity in short time intervals, between two consecutive images in time. It is expected that this variation between images pairs is most evident where there is fluctuation from time-varying speckle and, therefore, their sum must be substantially different in static and dynamic regions. The calculation is as follows:

$$Result_{i,j} = \sum_{t=1}^{N}\left|\left(I_{i,j,t} * I_{i,j,t-1}\right) - \left(I_{i,j,t}\right)^2\right| \quad (2)$$

The $Result_{i,j}$ is the final value calculated for a pixel with indexes *i, j*. The equation, thus, multiplies the intensity values of a given pixel at the instants t and t-1, consecutive, and subtracts the squared value of the intensity at time t. The resultant is a representative value of the variation seen for the pixel between times t and t-1. Only the absolute value is considered, because the important aspect is the fluctuation, be it positive or negative. It is easier to see the importance of variation in the calculation if we expand the equation (2), as follows:

$$Result_{i,j} = \sum_{t=1}^{N-1}\left|I_{i,j,t}\left(I_{i,j,t-1} - I_{i,j,t}\right)\right| \quad (3)$$

The term in parenthesis in equation (3) is the desired difference between the intensities, while the multiplicative term in evidence assists in the separation of background noise (usually low intensity) and signal (higher intensity). The proposed algorithm is then repeated for all pixels of a given image, generating one resulting image. The values are then normalized to the interval 0 - 255, from display. As in the case of SV, greater fluctuations result in brighter pixels (higher values) in such final image.

Both algorithms were implemented in the same development environment, using the same programming language – LabView (National Instruments, Austin, Texas, USA) -, same disk access methodology (the images are loaded into memory according to the iteration of the program), without any optimization and run on the same machine. This is necessary to enable the comparison of both approaches in terms of processing time.

3. RESULTS AND DISCUSSION

The first test performed consisted of whole milk being pumped into a Vena8 Fluoro+ microchannel, at a controlled flow rate. Together with the microchannel, in the original images, a cross section of a masking tape, glued to the surface of the Vena8 Fluoro, is visible. This acted as a static reference, in order to evaluate the performance of our method. An example of the original image can be seen in Figure 2.

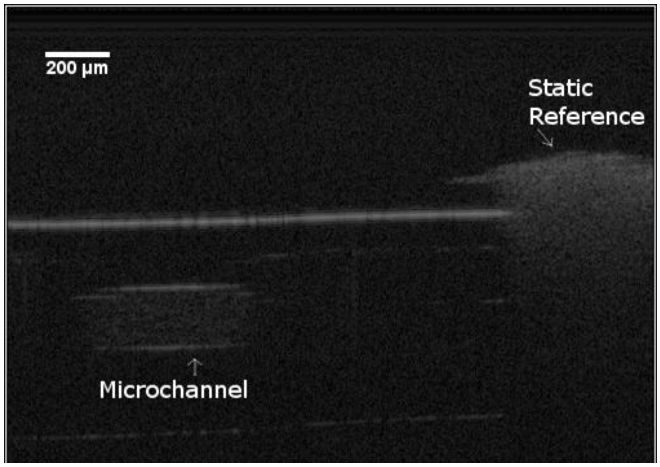

Figure 2. Example of an OCT image used for the tests, highlighting the microchannel and the static reference.

The milk was pumped at different flow rates, each being sampled and organized in different image sets. Each set consisted of 50 consecutive images, acquired at 8.6 images per seconds. The images were 500 x 500 pixels in dimension. The results obtained by our method, for the flow rates of 5 µl/min, 10 µl/min, 20 µl/min and 50 µl/min can be seen in Figure 3.

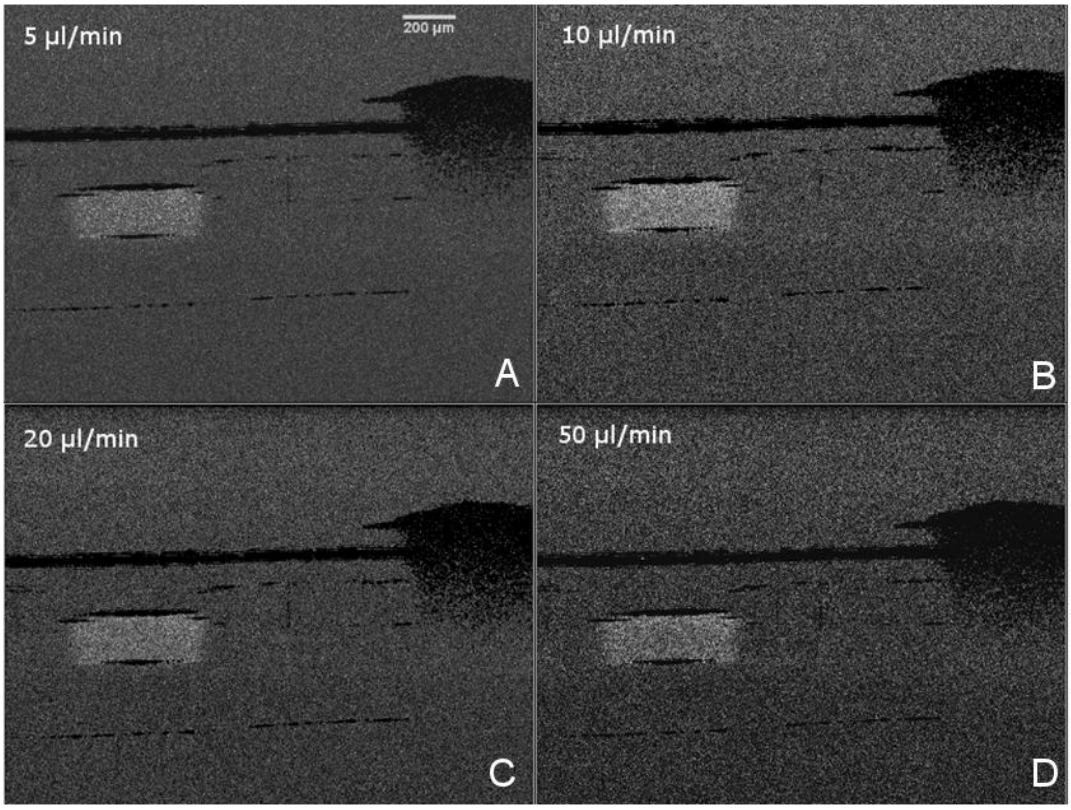

Figure 3. Results of our algorithm for the four flow rates tested. A)10 µl/min, B) 20 µl/min, C) 40 µl/min and D) 50 µl/min.

Two aspects are readily noticeable in all results. First, the static reference, as well as the microchannel chip surface and the upper and lower walls of the microchannel itself have all been blackened. This means that all those areas presented very little fluctuations over time, and the computed value is close to 0. This is expected from a region with static scatterers, as explained in section 2 of this work. This is a good indicator for the performance of the proposed method.

The second aspect to be noted is the microchannel area, which becomes pronounced in all results shown in Figure 3. The overall intensity of this region is in even greater in the computed images than in the original images. Once again, a positive result for the technique. This contrast between static and dynamic regions is the desirable outcome for the algorithm, just as it is for SV-OCT. This enables the mapping of flow for OCT images, which is the goal of the approach.

Also to be noted is the generally bright pixels presented in the background. As the images were acquired with no averaging (each image in the set is a single B-Scan), there's a strong presence of background noise, which also presents many fluctuations in intensity, which gives rise to this effect. However, the values for flow regions, for all flow rates, are higher, and thresholding can be utilized to further enhance visualization.

However, visually, it's not possible to discern between all the flow rates, with all the results being similar. The average value for the microchannel area was evaluated for each flow rate, for comparison. Each measurement was done by user input, selecting a rectangular area identified as the microchannel, and repeated five times. The results are in Figure 4.

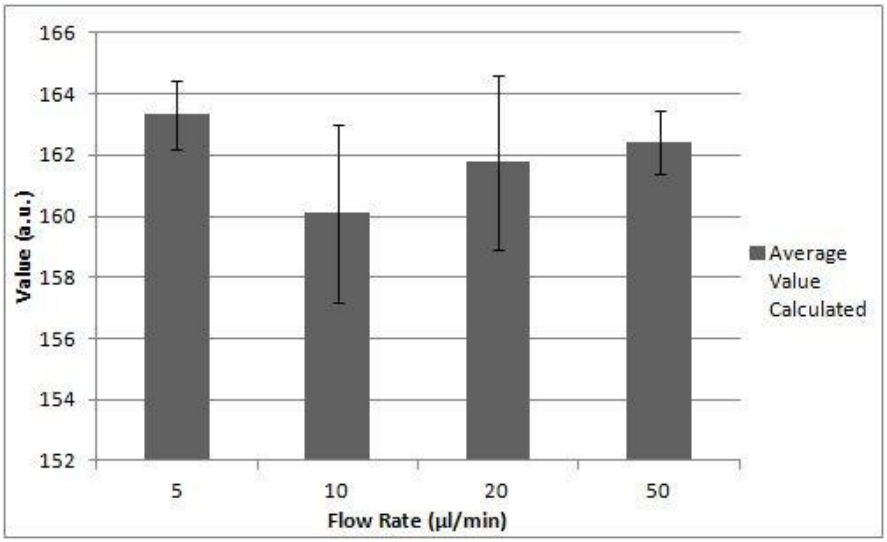

Figure 4. Comparison of the average value calculated for the microchannel region in different flow rates.

This results indicates that are no statistic difference between the values calculated for the flows, as well as there's no apparent relationship between those values and the flow rate. Just as the case of SV-OCT, it is not expected that this technique may be able to provide any quantitative information regarding the flow, serving only as a qualitative method. Therefore, the results in Figure 4 are not in disagreement with the objective of the approach.

Of special interest is the performance of the algorithm in terms of processing time. One of the proposed advantages for the new algorithm is the less complex calculation of the final values. In order to verify that, the same sets of images used to obtain the results shown in Figure 3 were subjected to SV-OCT algorithm. The processing times for both, our method and SV-OCT were noted. For each set of image, the computation was performed 5 times, totaling 20 tests. Figure 5 contains the results.

Our method performed better in every test, with comparable results. A gain of about 24% in processing time which, in this case, corresponds to a little over 1 second, was achieved. The main reason for that is the fact that our algorithm does not need previous knowledge of the average intensity over time for any pixels, while this is needed for SV-OCT. This makes the latter visit each frame two times, the first to compute the average and the second to compute the variance. In the proposed approach, each frame is loaded to the memory only once, and kept there for 2 consecutive iterations of the algorithm. However, the same amount of memory is used for both techniques, which is equivalent of three images. In the SV-OCT those are: 1) the current image in the iteration; 2) the Variance values and 3) the average intensity values. For our approach: 1) the first image in the iteration; 2) the second image in the iteration; 3) the final values computed. Therefore, the new algorithm has better computational performance than SV-OCT.

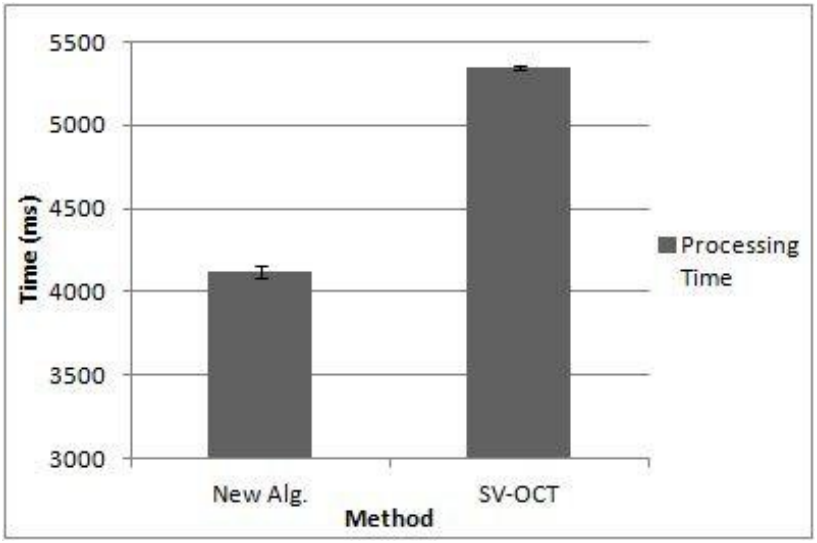

Figure 5. Comparison of processing times for the New Algorithm and SV-OCT.

As well as simulated flows, the new approach was also tested in a real biological application for evaluation of performance. For the input, B-Scans of the tip of a human index finger of a healthy subject were used. The set consisted of 50 images with dimensions of 512 x 512 pixels, acquired at 4.4 images per second. Each image is the average of two consecutive B-Scans, to suppress background noise artifacts. For this test, SV-OCT was used as the reference, and our results are compared to those obtained through SV. The Figure 6, contains an original image of the set, as well as both results.

In Figure 6-A, the original image is shown, and it can be noted that, without any computation, it is not possible to identify any zone as containing flow, with the whole signal inside the finger being similar. However, the same is not true for the results of SV-OCT (Figure 6-B) and the new method (Figure 6-C). In these results, static regions are darkened, and bright spots, identified as microcirculation, become evident. The spots identified in C are in good agreement with those in B, meaning that our approach has the same response as SV, a technique widely used in the literature, proving the new algorithm as capable of mapping flow with good accuracy. In C the average intensity of the whole finger region is higher, but the microcirculation spots are also higher in intensity, providing good contrast. Once again, the use of thresholding algorithms is viable.

It is valid to note that, in both results, it is possible to see a "trail" below the high intensity regions. This is known as Shadowing Effect or Shadowing Artifact and is related to how OCT acquires images[12], not being dependent on any posterior analysis performed.

As before, the processing times of both approaches are relevant to the comparison. For each algorithm, using the same set of 50 images of the index finger, 20 tests were performed, noting the processing time. The comparison can be seen in Figure 7. Again, our method performed better in every test, and obtained a gain of approximately 31% in processing time, corresponding to over 1.5 seconds. The same peak use of memory was observed.

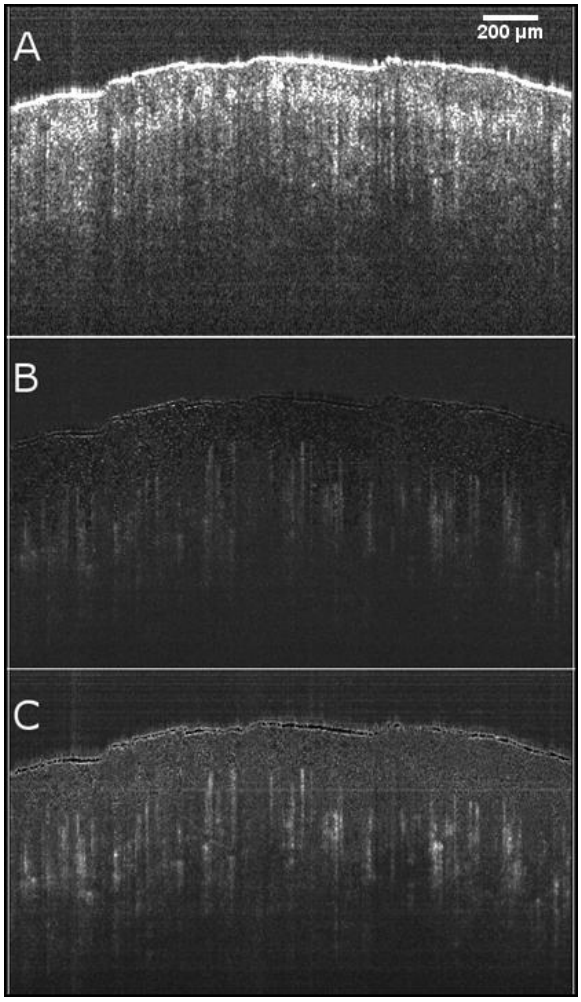

Figure 6. Comparison of the algorithms applied to a biological sample. A - Original image of the index finger. B – Result of SV. C - Result of the new algorithm.

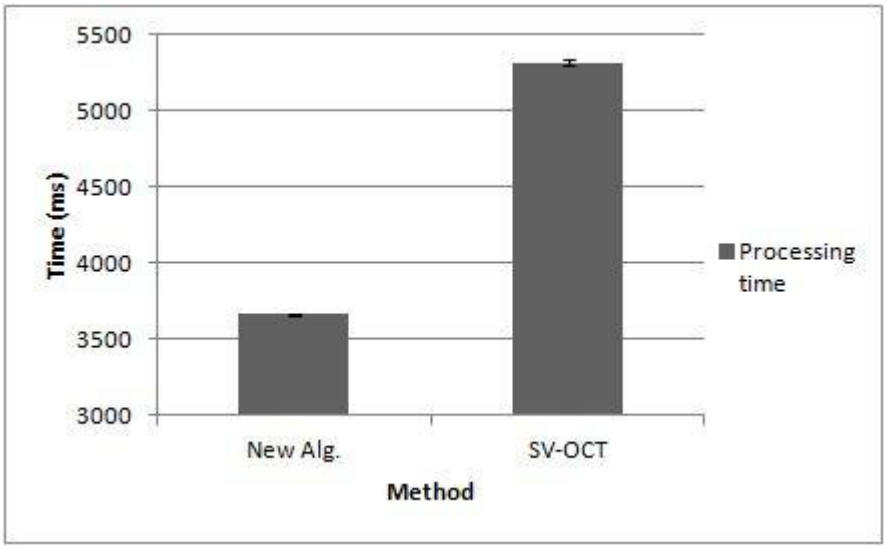

Figure 7. Comparison of processing times for both algorithms applied to a biological sample.

4. CONCLUSIONS

Through these tests it was possible to demonstrate and evaluate a new technique for flow visualization in OCT images, with good computational performance. It was demonstrated that, through observation of intensity fluctuation at short intervals (two consecutive frames) it is possible to differentiate static and moving regions, due to time-varying speckle.

It was shown that the proposed technique produces results that are in good agreement with those of SV-OCT, which is widely used in the literature. Also, the new algorithm has better performance when the processing time of both approaches are compared, being able to get results in shorter times in every test performed, achieving a gain as high as 31% in those tests. Both techniques have comparable memory usage.

Even though the proposed algorithm does not provide quantitative information, just as SV-OCT, it has many applications for vasculature imaging, and does not require any treatment of OCT images prior to the analysis, achieving good performance even when there's high background noise, as demonstrated. This makes the approach readily available to any set of OCT images acquired sequentially through time.

5. ACKNOWLEDGEMENTS

To FAPESP (Fundação de Amparo à Pesquisa do Estado de São Paulo, Project # 2013/05492-9 & # 2013/09311-9) for financial support.

REFERENCES

[1] Huang, D., Swanson, E. A., Lin, C. P., Schuman, J. S., Stinson, W. G., Chang, W., Hee, M. R., Flotte, T., Gregory, K., Puliafito, C. A., and Fujimoto, J. G., "OPTICAL COHERENCE TOMOGRAPHY," Science **254**, 1178-1181 (1991).

[2] Kodach, V. M., Kalkman, J., Faber, D. J., and van Leeuwen, T. G., "Quantitative comparison of the OCT imaging depth at 1300 nm and 1600 nm," Biomedical Optics Express **1**, 176-185 (2010).

[3] Schmitt, J. M., Xiang, S. H., and Yung, K. M., "Speckle in optical coherence tomography," Journal of Biomedical Optics **4**, 95-105 (1999).

[4] Du, Y. Z., Liu, G. J., Feng, G. Y., and Chen, Z. P., "Speckle reduction in optical coherence tomography images based on wave atoms," Journal of Biomedical Optics **19**, 7 (2014).

[5] Pircher, M., Gotzinger, E., Leitgeb, R., Fercher, A. F., and Hitzenberger, C. K., "Speckle reduction in optical coherence tomography by frequency compounding," Journal of Biomedical Optics **8**, 565-569 (2003).

[6] Bashkansky, M., and Reintjes, J., "Statistics and reduction of speckle in optical coherence tomography," Optics Letters **25**, 545-547 (2000).

[7] Mariampillai, A., Standish, B. A., Moriyama, E. H., Khurana, M., Munce, N. R., Leung, M. K. K., Jiang, J., Cable, A., Wilson, B. C., Vitkin, I. A., and Yang, V. X. D., "Speckle variance detection of microvasculature using swept-source optical coherence tomography," Optics Letters **33**, 1530-1532 (2008).

[8] Poole, K. M., McCormack, D. R., Patil, C. A., Duvall, C. L., and Skala, M. C., "Quantifying the vascular response to ischemia with speckle variance optical coherence tomography," Biomedical Optics Express **5**, 4118-4130 (2014).

[9] Cua, M., Lee, A. M. D., Lane, P. M., McWilliams, A., Shaipanich, T., MacAulay, C. E., Yang, V. X. D., and Lam S., "Lung vasculature imaging using speckle variance optical coherence tomography," Proc. SPIE 8207, 82073P1-82073P7 (2012).

[10] Sudheendran, N., Syed, S. H., Dickinson, M. E., Larina, I. V., and Larin, K. V., "Speckle variance OCT imaging of the vasculature in live mammalian embryos," Laser Physics Letters **8,** 247-252 (2011).

[11] Mariampillai, A., Leung, M. K. K., Jarvi, M., Standish, B. A., Lee, K., Wilson, B. C., Vitkin, A., and. Yang, V. X. D, "Optimized speckle variance OCT imaging of microvasculature," Optics Letters **35**, 1257-1259 (2010).

[12] Girard, M. J. A., Strouthidis, N. G., Ethier, C. R., and Mari, J. M., "Shadow Removal and Contrast Enhancement in Optical Coherence Tomography Images of the Human Optic Nerve Head," Investigative Ophthalmology & Visual Science **52**, 7738-7748 (2011).